THE JOURNAL OF BIOLOGICAL CHEMISTRY VOL. 287, NO. 13, pp. 10403–10413, March 23, 2012

Identification of NIPSNAP1 as a Nocistatin-interacting Protein Involving Pain Transmission*

Received for publication, June 14, 2011, and in revised form, January 20, 2012 Published, JBC Papers in Press, February 6, 2012, DOI 10.1074/jbc.M111.271866

Emiko Okuda-Ashitaka[‡§1], Toshiaki Minami[¶], Shingo Tsubouchi[‖], Hiroshi Kiyonari[**], Akihiro Iwamatsu[‡‡], Tetsuo Noda[§§], Hiroshi Handa[‖], and Seiji Ito[‡]

*From the [‡]Department of Medical Chemistry, Kansai Medical University, Moriguchi 570-8506, Japan, the [§]Department of Biomedical Engineering, Osaka Institute of Technology, Osaka 535-8585, Japan, the [¶]Department of Anesthesiology, Osaka Medical College, Takatsuki 569-8686, Japan, the [‖]Graduate School of Bioscience and Biotechnology, Tokyo Institute of Technology, Yokohama 226-8501, Japan, the **Laboratory for Animal Resources and Genetic Engineering, RIKEN Center for Developmental Biology, Kobe 650-0047, Japan, the [‡‡]Protein Research Network, Yokohama 236-0004, Japan, and the [§§]Department of Cell Biology, Japanese Foundation for Cancer Research, Cancer Institute, Tokyo 135-8550, Japan*

Background: Nocistatin (NST) is involved in pain transmission.
Results: 4-Nitrophenylphosphatase domain and non-neuronal SNAP25-like protein homolog 1 (NIPSNAP1) is purified by using NST-conjugated beads. The inhibition of tactile allodynia by NST is abolished in NIPSNAP1-deficient mice.
Conclusion: NIPSNAP1 interacts with NST and mediates pain modulation by NST.
Significance: These results may provide a novel therapeutic target for pathological pain.

4-Nitrophenylphosphatase domain and non-neuronal SNAP25-like protein homolog 1 (NIPSNAP1) is a molecule of physiologically unknown function, although it is predominantly expressed in the brain, spinal cord, liver, and kidney. We identified NIPSNAP1 as a protein that interacts with the neuropeptide nocistatin (NST) from synaptosomal membranes of mouse spinal cord using high-performance affinity latex beads. NST, which is produced from the same precursor protein as an opioid-like neuropeptide nociceptin/orphanin FQ (N/OFQ), has opposite effects on pain transmission evoked by N/OFQ. The calculated full-length pre-protein of NIPSNAP1 was 33 kDa, whereas the N-terminal truncated form of NIPSNAP1 (29 kDa) was ubiquitously expressed in the neuronal tissues, especially in synaptic membrane and mitochondria of brain. The 29-kDa NIPSNAP1 was distributed on the cell surface, and NST interacted with the 29-kDa but not the 33-kDa NIPSNAP1. Although intrathecal injection of N/OFQ induced tactile allodynia in both wild-type and NIPSNAP1-deficient mice, the inhibition of N/OFQ-evoked tactile allodynia by NST seen in wild-type mice was completely lacking in the deficient mice. These results suggest that NIPSNAP1 is an interacting molecule of NST and plays a crucial role in pain transmission.

4-Nitrophenylphosphatase domain and non-neuronal SNAP25-like protein homolog 1 (NIPSNAP1)[2] is a member of the NIPSNAP family consists of NIPSNAP1, NIPSNAP2, NIPSNAP3, and NIPSNAP4 (NIPSNAP3A); however, the physiological functions of the NIPSNAP protein family remain elusive. The gene for NIPSNAP1 in *Caenorhabditis elegans* is present in a polycistronic operon encoding 4-nitrophenylphosphatase and non-neuronal SNAP25-like proteins, and therefore it is thought to contribute to vesicular trafficking (1). NIPSNAP1 protein is expressed in the brain, spinal cord, liver, and kidney, and it has been reported to play several roles in the brain (2–5). NIPSNAP1 protein is localized in the postsynaptic density fraction of synapses, and its level is increased during generalized seizures caused by kainate (2). The level of NIPSNAP1 mRNA is reduced in the brain of a mouse model for phenylketonuria, an inborn error of amino acid metabolism caused by phenylalanine hydroxylase deficiency (3). NIPSNAP1, which localizes at mitochondria, binds to amyloid precursor protein that is implicated to Alzheimer disease (4), and the branched-chain α-ketoacid dehydrogenase enzyme complex that is disrupted in maple syrup urine disease (5). The physiological functions of NIPSNAP1 in the central nervous system remain unclear.

Recently, high-performance affinity latex beads, called SG beads, which are glycidylmethacrylate-covered glycidylmethacrylate-styrene copolymer core beads, have been used successfully to purify various proteins including drug receptors (6, 7). SG beads have a number of excellent features, such as low nonspecific protein interaction and high purification efficiency. In this study, we applied affinity chromatography using SG beads to identify nocistatin (NST)-interacting proteins for a better understanding of the molecular mechanism underlying the functions of NST. NST is a neuropeptide that is produced from the same precursor protein as nociceptin/orphanin FQ (N/OFQ), which is an opioid-like neuropeptide that selectively binds to the N/OFQ receptor, NOP (8–10). Although NST does not interfere with the binding of N/OFQ to NOP or N/OFQ-induced intracellular signaling *in vitro*, it blocks

* This work was supported in part by grants-in-aid for scientific research (S), (B), and (C) from the Japan Society for the Promotion of Science (to E. O.-A., T. M., and S. I.) and the Precursory Research for Embryonic Science and Technology (PRESTO) program from the Japan Science and Technology Agency (to E. O.-A.).

[1] To whom correspondence should be addressed: Osaka Institute of Technology, 5-16-1 Omiya, Asahi-ku, Osaka 535-8585, Japan. Tel.: 81-6-6954-4641; Fax: 81-6-6954-4649; E-mail: ashitaka@bme.oit.ac.jp.

[2] The abbreviations used are: NIPSNAP1, 4-nitrophenylphosphatase domain and non-neuronal SNAP25-like peotein homolog 1; N/OFQ, nociceptin/orphanin FQ; NOP, N/OFQ receptor; NST, nocistatin; TRPV, transient receptor potential vanilloid channel.

N/OFQ-induced pain transmission *in vivo* (8). NST itself exerts inhibitory effects, such as inflammatory pain responses (11–13) and morphine tolerance (14, 15). NST also induces pronociceptive effects in inflammatory pain response at high doses (nmol) (16, 17) and nociceptive flexor reflexes (18). In addition to pain transmission, NST is involved in other central nervous functions such as learning and memory (19), feeding (20), and anxiety (21, 22). Although the pharmacological functions of NST have been studied extensively, the precise molecular targets of NST and the mechanism(s) of pain regulation by NST remain unclear. Here, we identified NIPSNAP1, as an NST-interacting molecule, and demonstrated that NIPSNAP1 regulates pain transmission mediated by NST.

EXPERIMENTAL PROCEDURES

Affinity Purification of NST-interacting Proteins—Synaptosomal membranes were prepared from 4- to 5-week-old mice as described earlier (23). Briefly, mouse spinal cords in 10 mM Tris-HCl, pH 7.4, containing 0.32 M sucrose, 1 mM EDTA, 0.2 mM phenylmethylsulfonyl fluoride, and protease inhibitor mixture (Roche Applied Science) were homogenized with a Dounce homogenizer. The homogenate was centrifuged at 1,000 × *g* for 10 min at 4 °C, and the resulting postnuclear supernatant (S1) was centrifuged at 17,000 × *g* for 20 min to yield the crude synaptosomal and microsomal pellet (P2). The P2 pellet was resuspended in hypotonic buffer (5 mM Tris-HCl, pH 7.4, containing 0.5 mM EDTA), placed on ice for 30 min, and centrifuged at 25,000 × *g* for 30 min to yield the synaptosomal membrane (LP1). The LP1 was dissolved in lysis buffer containing 0.3% *n*-octyl-β-thioglucoside, 10 mM Tris-HCl, pH 7.4, 1 mM EDTA, 10 mM $MgCl_2$, 25% glycerol, 1 mM DTT, and protease inhibitor mixture at 4 °C for 1 h, and then centrifuged at 100,000 × *g* for 30 min. The resultant supernatant was incubated at 4 °C for 16 h with NST-immobilized SG beads (concentration of conjugated NST: 0, 1.2, 2.9, and 4.8 μM) in the presence or absence of 10 μM NST. NST-immobilized SG beads were prepared as described previously (6). After the beads had been washed with the lysis buffer, the bound proteins were eluted with 1 M NaCl. The bound proteins were subjected to SDS-PAGE and silver staining. For analysis of mass spectrometry, the proteins were transferred to polyvinylidene difluoride filters (Applied Biosystems) and then stained with colloidal gold (Bio-Rad). The stained bands were subjected to in-gel trypsin digestion, and the resultant peptides were analyzed by matrix-assisted laser desorption/ionization time-of-flight mass spectrometry.

Isolation of NIPSNAP and NOP cDNAs—The cDNAs encoding NIPSNAP1, NIPSNAP2, and NIPSNAP3A (annotated as NIPSNAP4) were amplified using polymerase chain reaction (PCR) with cDNAs synthesized from mouse spinal cord mRNAs. The nucleotide sequences obtained were identical to those of NIPSNAP1 (accession number NM_008698), NIPSNAP2 (NM_008095), and NIPSNAP3A (NM_025623). cDNA encoding NOP was generated by PCR from a human brain cDNA library (accession number X_77130). The cDNAs were subcloned into pEF-Bos (kindly donated by Shigekazu Nagata, Kyoto University, Kyoto, Japan) for expression. The C-terminal hemagglutinin (HA)-tagged NIPSNAP1 (NIPSNAP1-HA) and the N-terminal HA-tagged nociceptin receptor (NOP-HA) were constructed using pCG-C-BL and pCG-N-BL (provided by Jun-ichi Fujisawa, Kansai Medical University, Osaka, Japan), respectively.

Cell Cultures and Transfections—COS-7 cells were grown under 5% CO_2 at 37 °C in Dulbecco's modified Eagle's medium (Invitrogen) containing 10% fetal calf serum, 100 units/ml of penicillin, and 100 μg/ml of streptomycin. cDNA transfection was performed by using Lipofectamine (Invitrogen) according to the manufacturer's instruction.

Antibodies—Anti-NIPSNAP1 antibody was obtained by immunization of rabbits with keyhole limpet-coupled synthetic peptides (anti-NSP1-N, MAPLCIISAAARRL; anti-NSP1-I, SLTEAVLPKLHLDEDYPCS; and anti-NSP1-C, LVRHMESRIMIPLKISPLQ) according to the method described previously (8). Anti-NSP1-N and anti-NSP1-I antibodies recognized specifically NIPSNAP1, but anti-NSP1-C antibody cross-reacted with NIPSNAP2 (Fig. 2*B*). Other primary antibodies used in this study were as follow: mouse anti-β-tubulin (1:1,000; Sigma), rabbit anti-NR2B (1:500; Chemicon), mouse anti-synaptophysin (1:2,000; BD Bioscience), mouse anti-heat shock protein (HSP) 60 (1:300; Chemicon), rabbit anti-HA (1:1,000; NeoMarkers), and rabbit anti-NST (0.5 μg/ml; Okuda-Ashitaka *et al.* (11)). The secondary antibodies were horseradish peroxidase (HRP)-conjugated sheep anti-mouse IgG (1:10,000; GE Healthcare UK Ltd.), HRP-conjugated goat anti-rabbit IgG (1:20,000; BIOSOURCE), Alexa 546-conjugated goat anti-rabbit IgG (1:500, Molecular Probes), and Alexa 488-conjugated goat anti-mouse IgG (1:500, Molecular Probes). NeuroTrace Fluorescent Nissle stain (1:150) was from Molecular Probes.

Immunoblotting—Subcellular fractions of mouse brain were performed as described previously (24). Protein samples were quantified by using a Bradford protein assay (Bio-Rad). Proteins were loaded into the SDS-PAGE gel, electrophoresed, and transferred electrophoretically to polyvinylidene difluoride membranes (Bio-Rad). After having been blocked for 1 h at room temperature with 3% skim milk in a TBS-T buffer containing 0.1% Triton X-100, 150 mM NaCl, and 10 mM Tris-HCl, pH 7.4, the membrane was incubated with primary antibodies and secondary antibodies conjugated to horseradish peroxidase. Signals were detected with an enhanced chemiluminescence system (GE Healthcare UK Ltd.). The intensity of immunostaining was quantified by use of ImageJ.

Immunochemistry—NIPSNAP1-transfected COS-7 cells grown on poly-L-lysine-coated glass dishes were fixed with 4% paraformaldehyde for 10 min at room temperature and subsequently incubated in the presence (permeabilizing condition) or absence (non-permeabilizing condition) of 0.3% Triton X-100 for 15 min. After having been washed with PBS, the cells were blocked with PBS containing 2% normal goat serum and 1% bovine serum albumin, and incubated with primary antibodies overnight. Immune complexes were visualized with Alexa 546- and Alexa 488-labeled secondary antibodies. Immunohistochemistry was carried out as described previously (8). Digital images were captured by a Zeiss laser-scanning confocal microscope LSM510 equipped with argon (at 488 nm for Alexa Fluor 488) and HeNe1 (at 543 nm for Alexa Fluor 546) lasers and the appropriate filters. Samples of a set of control and

experimental cells and tissues were concurrently immunostained, and images were captured under the same conditions.

[^{3}H]NST Binding—[^{3}H]NST binding was used with aliquots of the same crude membrane prepared from NIPSNAP1-transfected cells. The crude membranes prepared from NIPSNAP1-transfected COS-7 cells and mouse spinal cord were incubated for the indicated times at 4 or 30 °C for time and temperature dependence, and for 60 min at 30 °C for saturation binding, with [^{3}H]NST (Phoenix Pharmaceuticals, Inc.) in buffer containing 50 mM Tris-HCl, pH 7.4, 10 mM $MgCl_2$, 1 mM EDTA, 500 μg/ml of protease-free bovine serum albumin, 100 μg/ml of bacitracin, and 10 μg/ml of pepstatin A. After the incubation, the reaction mixtures were applied to a Whatman GF/C glass filter pretreated with 0.3% polyethylenimine. The filter was then washed three times with 50 mM Tris-HCl, pH 7.4, and 1 mM EDTA, and the radioactivity was counted by a scintillation counter. Nonspecific binding was determined by using unlabeled NST (10 μM) in the reaction mixture. The specific binding was calculated by subtracting the nonspecific binding from the total binding.

Immunoprecipitation—The COS-7 cells expressing NIPSNAP1-HA and NOP-HA were dissolved in the same lysis buffer for affinity purification of NST-interacting proteins, and then centrifuged at 20,000 × *g* for 20 min. The protein concentration of the resultant supernatant was determined with a DC protein assay (Bio-Rad). The cell lysate was incubated at 30 °C for 1 h with [^{3}H]NST (15 nM), and then for 1 h with anti-HA-conjugated agarose (Sigma). After the incubation, the reaction mixtures were applied to a Whatman GF/C glass filter pretreated with 0.3% polyethylenimine. The filter was then washed three times with 50 mM Tris-HCl, pH 7.4, and 1 mM EDTA, and the radioactivity was counted in a scintillation counter.

Surface Biotinylation Assay—NIPSNAP1-transfected COS-7 cells were labeled for 1 h at 4 °C with 1 mg/ml of Sulfo-NHM-LC-Biotin (Pierce) in Dulbecco's PBS containing 0.5 mM $MgCl_2$ and 0.9 mM $CaCl_2$ (PBS(+)). Unreacted biotinylation reagent was quenched by two washes with a solution of ice-cold PBS(+) containing 100 mM glycine and a subsequent 30-min incubation in the same solution. After three additional washes in ice-cold PBS(+), the cells were lysed in lysis buffer (10 mM Tris-HCl, pH 7.4, containing 140 mM NaCl, 0.3% *n*-octyl-β-thioglucoside, 0.2 mM sodium orthovanadate, and protease inhibitor mixture), and centrifuged at 20,000 × *g* for 15 min at 4 °C. The supernatants containing equal amounts of proteins were incubated with NeutraAvidin-agarose (Pierce) overnight to immunoprecipitate the surface-biotinylated proteins. After five washes in lysis buffer, precipitated proteins were eluted from the streptavidin beads by boiling in reducing sample buffer and then analyzed by immunoblotting.

Generation of NIPSNAP1 Mutant Mice—The NIPSNAP1 mutant (RIKEN accession number CDB0535K) was established as follows: NIPSNAP1-deficient mice were generated by the gene targeting technique described previously (25). NIPSNAP1 was isolated from a C57BL/6 mouse bacterial artificial chromosome gene library. We constructed a targeting vector by inserting a neomycin-resistance cassette into the NIPSNAP1 locus (exon II–IV). To generate NIPSNAP1-deficient mice, we transfected TT2 embryonic stem cells with the targeting vector, and then screened G418-resistant clones for homologus recombination by PCR and Southern blot analysis (26). Embryonic stem clones carrying the targeted NIPSNAP1 allele were introduced into host embryos and used to produce chimeric mice. The chimeras with a high embryonic stem cell contribution were crossed with C57BL/6 mice to produce NIPSNAP1$^{+/-}$ mice. NIPSNAP1$^{-/-}$ mice were generated by intercrossing of the NIPSNAP1$^{+/-}$ mice. The genotype of the mice were determined by PCR using primers (5′-GCTGTACTGCCCAAGCTGCACCTG-3′, 5′-CGCATCGCCTTCTATCGCCTTCTT-3′, and 5′-GAGAGAGGAGGGCAGACAGATACG-3′). The length of the amplified fragments were 174 bp for wild-type and 483 bp for the mutant. For Southern blot analysis, genomic DNA was digested with NheI, separated by electrophoresis through a 0.8% agarose gel, and transferred to a nylon membrane. For hybridization we used a 968-bp DNA fragment located outside the targeting vector. The protocols used for all animal experiments in this study were approved by the Animal Research Committee of Kansai Medical University and RIKEN Kobe Animal Experiment Committee.

Behavioral Analysis—Animal experiments were carried out in accordance with the National Institutes of Health guide for the care and use of laboratory animals and the ethical guidelines of the Ethics Committee of the International Association for the Study of Pain (27). NIPSNAP1$^{-/-}$ mice and their cognate wild-type mice were obtained from respective heterozygous breeding pairs of mice. Eight to 12-week-old male mice were used for behavioral analyses. Tactile allodynia was assessed once every 5 min for 50 min by light stroking of the flank of the mice with a paintbrush after intrathecal injection of NST and/or N/OFQ into the subarachnoid space between the L5 and L6 vertebrae (8, 28). The allodynic response was ranked as follows: 0, no response; 1, mild squeaking with attempts to move away from the stroking probe; 2, vigorous squeaking evoked by the stroking probe, biting at the probe, or strong efforts to escape. The maximum possible scores for allodynia of 6 mice were 2 × 6 = 12 in any 5-min period and 2 × 6 ×20 = 120 for 50 min, and either was taken as 100%.

Chemicals—NST was kindly provided from Yuji Nishiuchi, Peptide Institute, Minoh, Japan.

Statistical Analysis—All data were expressed as the mean ± S.E. We evaluated statistical significance with Student's *t* test or the Mann-Whitney *U* test for comparisons between two mean values.

RESULTS

Identification of NIPSNAP1 as an NST-interacting Protein—To identify molecules that interact with NST, we performed affinity purification using NST-conjugated SG beads, which have been successfully used as an affinity resin showing minimal nonspecific interactions. We tried to isolate NST-interacting proteins from the extract of synaptosomal membranes in mouse spinal cord solubilized with 0.3% *n*-octyl-β-D-thioglucoside. Although most protein bands were decreased by 7–30% in the presence of free NST (10 μM), the 29-kDa protein by 91%, the 28-kDa protein by 38%, and the 27-kDa protein by 63%. Three proteins with apparent molecular mass of ~29, 28, and

27 kDa interacted with the NST-conjugated SG beads in a concentration-dependent manner (Fig. 1, *A* and *B*). These proteins did not bind to control beads; and their band density decreased in the presence of an excess amount of free NST, but not N/OFQ (Fig. 1*C*), suggesting that the interaction between these proteins and NST-conjugated SG beads was specific. Mouse NIPSNAP1 (accession number NP 032724.1; Fig. 1*E*) was identified by mass spectral analysis of these proteins. To confirm the

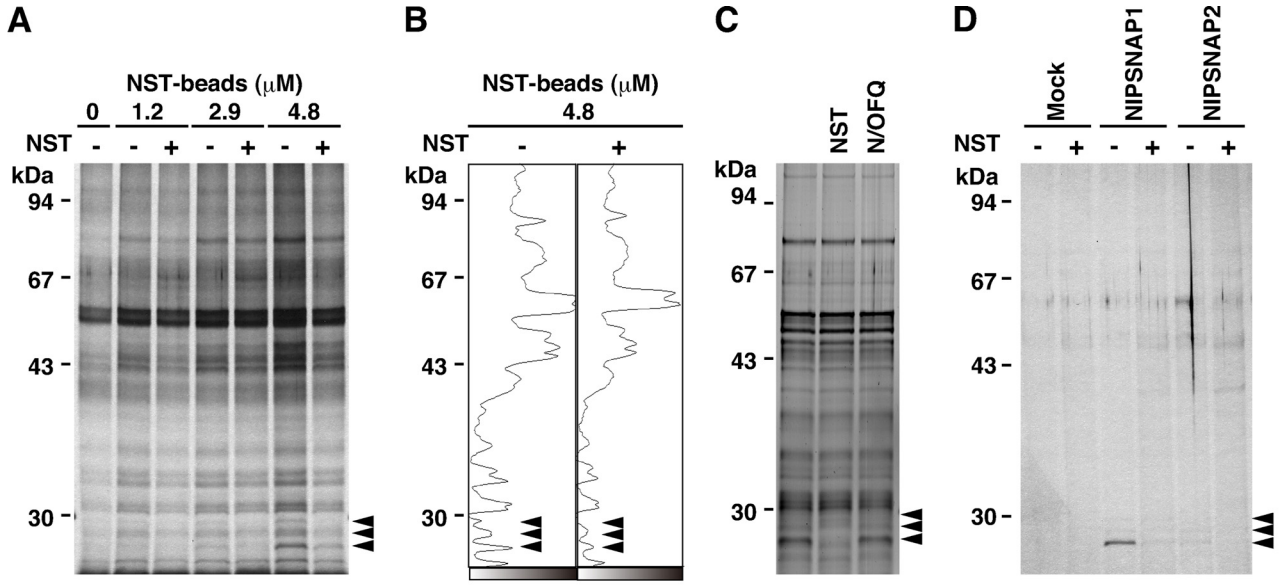

E

```
                                  α-NSP1-N
NIPSNAP1      1  MAPRLCIISAAARRLFTKPRPRAGDLAAAGAVRFYSKDSEGSWFRSLFVHKVDPRKDAHS  60
NIPSNAP2      1  MAAR---VLLARGGLLRPAAQSAFLPGLRTVTSSSHRARPDSWLKSLFVRKVDPRKDAHS  57
NIPSNAP3A     1  MLALRSGLRTALAPRVLTPQVC-------------------------------------S  23
                                                  α-NSP1-I
NIPSNAP1     61  TLLSKKETSNLYKIQFHNVKPECLDAYNSLTEAVLPKLHLDEDYPCSLVGNWNTWYGEQD  120
NIPSNAP2     58  NLLAKKETSSLYKLQFHNVKPECLDAYNKICQEVLPKIHEGKQYPCTLVGTWNTWYGEQD  117
NIPSNAP3A    24  PFATGPRQSNGTFYEFRTYFLKPSKTNEFLENFKNSVHLRTAHSEMIGYWLVEFGGRTNR  83

NIPSNAP1    121  QAVHLWRFSGGYPALMDCMNKLKNNKEYLEFRKERSKMLLSRRNQLLLEFSFWNEPQPRA  180
NIPSNAP2    118  QAVHLWRYEGGYPALTEVMNKLKENQEFVNFRKAASDMLLSRKNQLLLEFSFWNEPVPRP  177
NIPSNAP3A    84  VFHIWKYDNFAHRTAVRKALAKDKEWQERFLIPNLAFIDKQEVEITYLVPWCKIGTPPKE  143

NIPSNAP1    181  GPNIYELRTYKLKPGTMIEWGNNWARAIKYRQENQEAVGGFFSQIGELYVVHHLWAYKDL  240
NIPSNAP2    178  GPNIYELRSYQLRPGTMIEWGNYWARAIRFRQDSNEATGGFFSQIGQLYMVDHLWAYRDL  237
NIPSNAP3A   144  GVYELATFQMKPGGPALWGNAFKRAVNAHVELGYSTLVGVFHTEYGALNRVHVLWWNESA  203
                                  α-NSP1-C
NIPSNAP1    241  QSREETRNAAWRKRGWDENVYYTVPLVRHMESRIMIPLKISPLQ                  284
NIPSNAP2    238  QTREDIRNAAWHKHGWEELVYYTVPLIQEMESRIMIPLKTSPLQ                  281
NIPSNAP3A   204  DSRAAGRHWSHEDPRVVAAVRESVSYLESQQNTFLLPTSFSPLK                  247
```

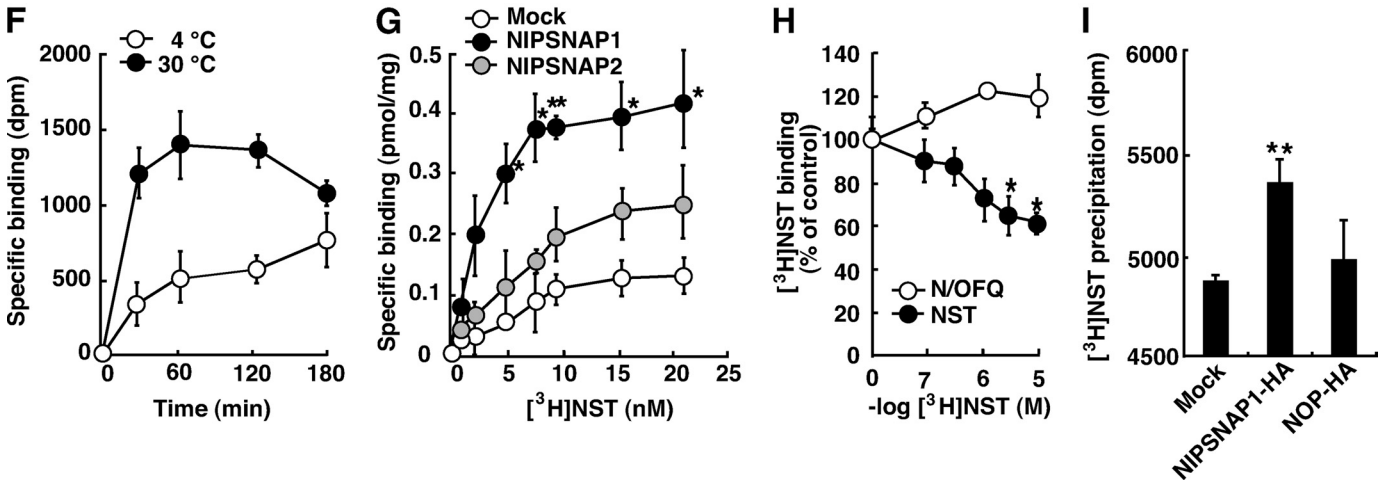

interaction between these proteins and NST-conjugated SG beads, we cloned NIPSNAP1 cDNA from mouse spinal cord, and used expression vectors encoding the cDNA for transfection of COS-7 cells. By the same affinity purification procedure using NST-conjugated SG beads, two faint bands (~29 and 28 kDa) and one strong band (~27 kDa) were evidently detected on silver-stained SDS-PAGE gels when an extract from the membranes of COS-7 cells expressing NIPSNAP1 was examined (Fig. 1*D*). A highly homologous protein of NIPSNAP1, NIPSNAP2 (also called glioblastoma amplified sequence; accession number NP 03212.1), could not be purified by use of the NST-conjugated SG beads. To further confirm the interaction of NIPSNAP1 with NST, we carried out a binding assay using [^{3}H]NST. [^{3}H]NST bound to the membrane fraction of NIPSNAP1-transfected COS-7 cells, and the [^{3}H]NST binding was higher at 30 °C than at 4 °C, and reached equilibrium after 60 min at 30 °C (Fig. 1*F*). When the NIPSNAP1-expressing COS-7 cell membrane was incubated for 60 min at 30 °C with increasing concentrations of [^{3}H]NST (1.1–22.0 nM), [^{3}H]NST significantly bound to the membrane fraction of NIPSNAP1-transfected cells (Fig. 1*G*). Scatchard plot analysis of the specific binding to NIPSNAP1 revealed a high-affinity binding site (K_d 5.8 nM, 0.67 pmol/mg of protein). [^{3}H]NST tended to bind to NIPSNAP2, but not significantly, and a slight binding was found in the membrane of the mock-transfected cells. The binding to [^{3}H]NST (15 nM) was displaced by unlabeled NST, but not N/OFQ, in a concentration-dependent manner (Fig. 1*H*). Furthermore, we carried out co-immunoprecipitation of [^{3}H]NST with the C-terminal HA-tagged NIPSNAP1 (NIPSNAP1-HA) and the N-terminal HA-tagged nociceptin receptor (NOP-HA). NIPSNAP1-HA and NOP-HA expressed in COS-7 cells were immunoprecipitated with anti-HA-conjugated agarose and subjected to a Whatman GF/C filter. [^{3}H]NST significantly bound NIPSNAP1-HA, but not NOP-HA (Fig. 1*I*).

The predicted protein from NIPSNAP1 cDNA consisted of 284 amino acid residues with a calculated molecular weight of 33,363. Although seven peptide sequences obtained by mass spectral analysis were found within the deduced amino acid sequence (Fig. 1*E*), there were no peptide fragments close to the N and C termini of NIPSNAP1 among the peptide fragments. We characterized NIPSNAP1 by using anti-NIPSNAP1 antibodies that recognized the N-terminal region (anti-NSP1-N) and the C-terminal region (anti-NSP1-C; Figs. 1*E* and 2*A*). A 33-kDa protein was detected by both anti-NSP1-N and anti-NSP1-C antibodies

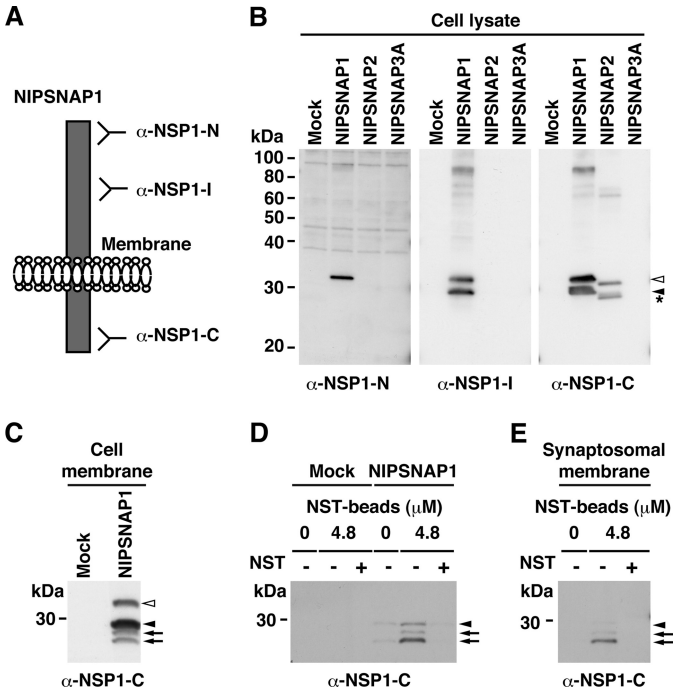

FIGURE 2. **Characterization of NIPSNAP1 protein.** *A*, schematic diagram depicting the structure and antibodies against NIPSNAP1. *B*, specificity of NIPSNAP1 antibodies. COS-7 cells expressing NIPSNAP1, NIPSNAP2, or NIPSNAP3A were subjected to immunoblot analysis with anti-NSP1-N, anti-NSP1-I, and anti-NSP1-C antibodies. *C*, immunoblotting of the membrane fraction of NIPSNAP1-transfected COS-7 cells with anti-NSP1-C antibody. *D* and *E*, immunoblotting of the eluates from COS-7 cells transfected with NIPSNAP1 in Fig. 1*D* (*D*) and synaptosomal membrane extracts of the spinal cord in Fig. 1*A* (*E*) with anti-NSP1-C antibody. These experiments were performed at least 4 times, and similar results were obtained. The *open arrowheads* indicate the full-length form of NIPSNAP1 (*B* and *C*); the *closed arrowhead* indicate a mature form of NIPSNAP1 (*B–E*). The *asterisk* indicate NIPSNAP1 (*B*). *Arrows* indicate NIPSNAP1-related proteins (*C–E*).

(Fig. 2*B*), suggesting it to be full-length NIPSNAP1. The 29-kDa protein of NIPSNAP1 was detected by anti-NSP1-C, but not by anti-NSP1-N. This protein was truncated at the N-terminal region of NIPSNAP1. Although four bands of ~33-, 29-, 28-, and 27-kDa proteins were detected in the extract of the membrane of NIPSNAP1-expressing COS-7 cells by anti-NSP1-C (Fig. 2*C*), the 33-kDa protein was not detected with NST-conjugated SG beads (Fig. 2*D*). Immunoblot analysis using anti-NSP1-C antibody showed two faint bands (~29 and 28 kDa) and one strong band (~27 kDa) in the affinity purified eluate from the extract of synaptosomal membranes of mouse spinal cord (Fig. 2*E*). The surface biotinylation assay using the membrane protein NOP-HA and mito-

FIGURE 1. **Purification and identification of NST-interacting proteins.** *A*, NST-conjugated SG beads at the indicated concentrations of NST and unconjugated SG beads were incubated overnight at 4 °C with synaptosomal membrane extracts of the spinal cord. *B*, quantification of protein bands in the *right two lanes* of *A* (NST-beads 4.8 μM with or without NST) using ImageJ. *C*, displacement of NST-conjugated SG beads binding protein bands by 10 μM NST and 10 μM N/OFQ. *D*, proteins from COS-7 cells transfected with expression vectors for mouse NIPSNAP1 and NIPSNAP2 were purified with NST-conjugated SG beads. The eluates were subjected to SDS-PAGE followed by silver staining. These experiments were performed at least 4 times, and similar results were obtained. *Arrowheads* in *A–D* indicate the positions of the interacting proteins. *E*, amino acid sequences of mouse NIPSNAP1, NIPSNAP2, and NIPSNAP3A. The parts of NIPSNAP1 in *red* correspond to the peptide fragments obtained by trypsin digestion. The peptide fragments used as immunogens are indicated by the *blue underlines*. Conserved residues are *boxed*. A possible transmembrane helix is *shadow boxed*. *F–I*, [^{3}H]NST binding to NIPSNAP1. *F*, the membrane fraction prepared from COS-7 cells expressing mouse NIPSNAP1 was incubated with [^{3}H]NST (8 nM) at 4 and 30 °C. Specific binding was determined as described under "Experimental Procedures." Data are expressed as the mean ± S.E. (n = 3–6). *G*, the membrane fractions prepared from COS-7 cells expressing mouse NIPSNAP1 and NIPSNAP2 were incubated with the indicated concentrations of [^{3}H]NST at 30 °C. Data are expressed as the mean ± S.E. (n = 3–9). **, $p < 0.01$; *, $p < 0.05$ *versus* vector-transfected cells (mock). *H*, [^{3}H]NST (15 nM) binding was determined in the presence of the indicated concentrations of unlabeled NST or N/OFQ (mean ± S.E., n = 3). *, $p < 0.05$ *versus* vehicle. *I*, NIPSNAP1-HA and NOP-HA expressed in COS-7 cells were immunoprecipitated with anti-HA antibody-conjugated agarose and applied to a Whatman GF/C filter. Data are expressed as the mean ± S.E. (n = 3). **, $p < 0.01$ *versus* mock.

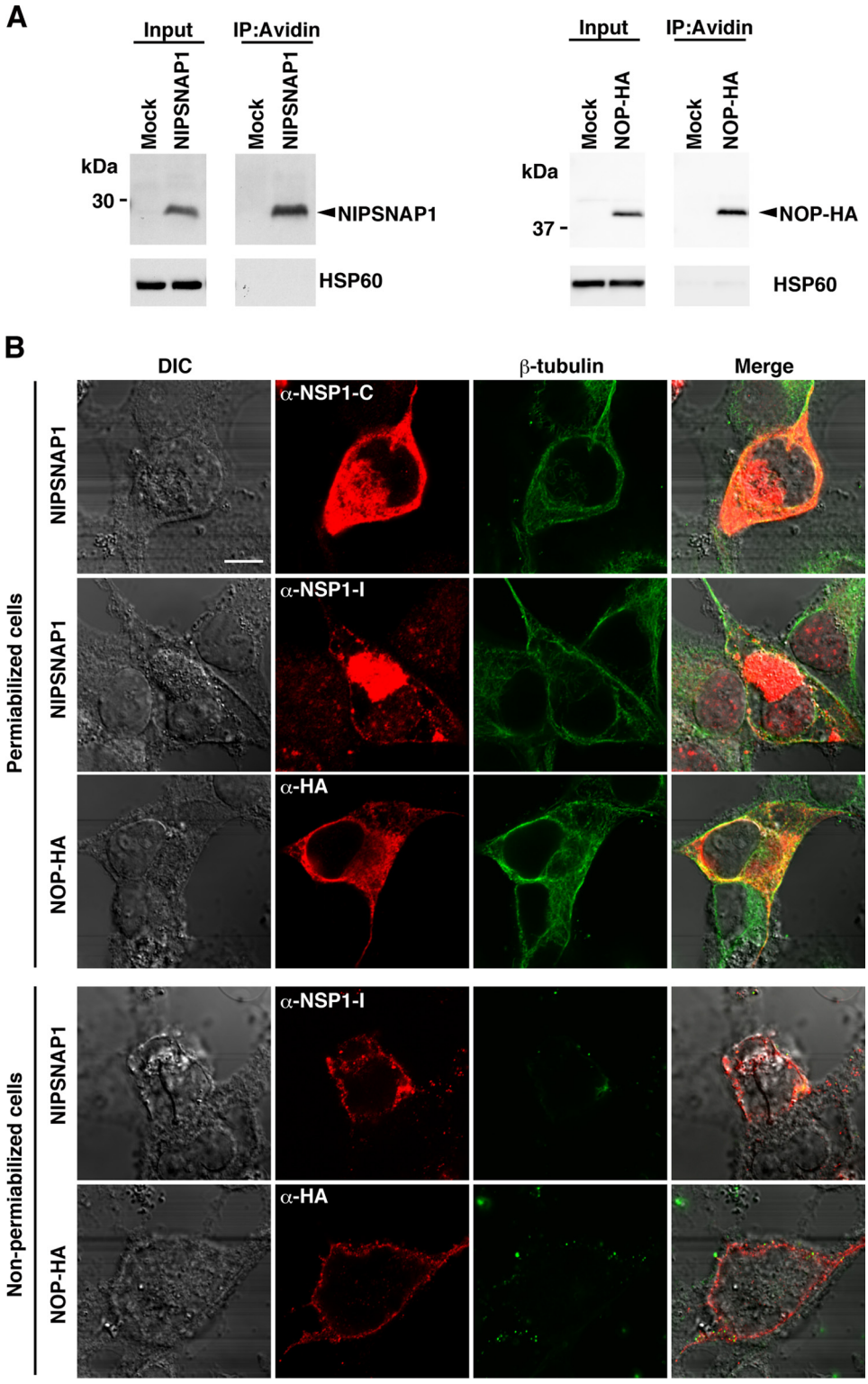

FIGURE 3. **Cell surface expression of NIPSNAP1.** *A*, total and surface levels of NIPSNAP1 and NOP were examined in NIPSNAP1- and NOP-HA-transfected COS-7 cells by using biotinylation and immunoblot analysis with anti-NSP1-C, anti-HA, and anti-HSP60 antibodies. *B*, immunofluorescence analysis using anti-NSP1-I, anti-NSP1-C, anti-HA, and anti-β-tubulin antibodies with permeablized and non-permeablized NIPSNAP1- and NOP-HA-transfected COS-7 cells. These experiments were performed at least 3 times, and similar results were obtained. *Bar*, 10 μm.

chondrial HSP60 as positive and negative controls, respectively, revealed that the 29-kDa NIPSNAP1 and NOP-HA, but not HSP60, were labeled with a membrane-impermeable biotinylating reagent (Fig. 3*A*). Furthermore, immunofluorescence was observed with both anti-NSP1-I (raised against the intermediate region of NIPSNAP1) and anti-NSP1-C antibodies in fixed- and permeabilized-COS-7 cells expressing NIPSNAP1, similar to NOP-HA and a cytoskeleton protein β-tubulin (Fig. 3*B*). In the fixed- and non-permeabilized cells, immunofluorescence at the cell periphery was detected

with anti-NSP1-I and anti-HA, but not anti-β-tubulin. These results suggest that 29-kDa NIPSNAP1 was expressed on the cell surface.

Expression of 29-kDa Protein of NIPSNAP1 as Mature Form—We examined the expression of NIPSNAP1 protein by immunoblot analysis using anti-NSP1-I and anti-NSP1-C antibodies. Anti-NSP1-I antibody specifically recognized NIPSNAP1, whereas anti-NSP1-C antibody recognized both NIPSNAP1 and NIPSNAP2 (Fig. 2*B*). Immunoblot analysis using the anti-NSP1-I antibody revealed that the 29-kDa protein was distributed in the brain, spinal cord, liver, and kidney (Fig. 4*A*). Similarly, this protein was also detected in these tissues with anti-NSP1-C antibody. These results indicate that the 29-kDa protein is the mature form of NIPSNAP1 *in vivo*. The mature form of NIPSNAP1 was distributed in various brain regions (Fig. 4*B*). Furthermore, subcellular distribution analysis of the brain showed that the mature form of NIPSNAP1 was relatively concentrated in the synaptic membrane and mitochondrial fractions, which fractions were confirmed by the detection of *N*-methyl-D-aspartate (NMDA) receptor subunit NR2B and HSP60, respectively (Fig. 4*C*). The mature form of NIPSNAP1 was hardly detected in the synaptic vesicle fraction, which was confirmed by the presence of synaptophysin. These results suggest that the 29-kDa protein of NIPSNAP1 is the mature form that is detected ubiquitously in various brain regions and the spinal cord and is concentrated in the synaptic membrane and mitochondrial fractions.

NIPSNAP1-deficient Mice—To determine the pathophysiological role of NIPSNAP1 in pain transmission, we disrupted the mouse gene by homologous recombination in embryonic stem cells (Fig. 5*A*). We used Southern blot analysis of NheI-digested genomic DNA and PCR of genomic DNA to ensure proper targeting (Fig. 5, *B* and *C*). NIPSNAP1$^{-/-}$ mice were obtained at the expected Mendelian frequency and were fertile. Whereas wild-type brain, spinal cord, liver, and kidney exhibited the 29-kDa NIPSNAP1 protein band, no NIPSNAP1 protein bands were detected in the NIPSNAP1$^{-/-}$ mice (Fig. 5*D*). Also, specific [^{3}H]NST binding was significantly reduced in the spinal cord membrane fraction of NIPSNAP1$^{-/-}$ mice (Fig. 5*E*). NIPSNAP1$^{-/-}$ mice exhibited no gross histological abnormalities of the spinal cord by Nissl staining (Fig. 5*F*). Furthermore, NIPSNAP1$^{-/-}$ mice exhibited no difference of the spinal cord in reactivity with anti-NST antibody, similar to the intensity of wild-type mice (Fig. 5*G*).

Involvement of NIPSNAP1 in Inhibition of N/OFQ-evoked Tactile Allodynia by NST—Intrathecal injection of NST blocks the N/OFQ-induced allodynia, a pain response to tactile stimuli applied to the flank with a paint brush (8). To address how NIPSNAP1 affected pain regulation by NST, we analyzed tactile allodynia on NIPSNAP1$^{-/-}$ mice. Allodynia was strongly evoked by the first stimulus at 5 min after the intrathecal injection of 50 pg of N/OFQ and was observed by tactile stimulation every 5 min for 50 min in both NIPSNAP1$^{-/-}$ and wild-type mice (Fig. 6*A*). NST (500 pg/mouse) alone did not induce allodynia in either NIPSNAP1$^{-/-}$ or wild-type mice. Although simultaneous intrathecal injection of N/OFQ and NST significantly inhibited N/OFQ-induced allodynia over the 50-min experiment in wild-type mice, the N/OFQ-evoked allodynia was not blocked by NST in the NIPSNAP1$^{-/-}$ mice (Fig. 6*B*). When the scores of allodynia obtained for the overall 50 min were cumulated, the N/OFQ (50 pg/mouse)-induced allodynia was dose-dependently inhibited by NST at 5 and 50 pg in

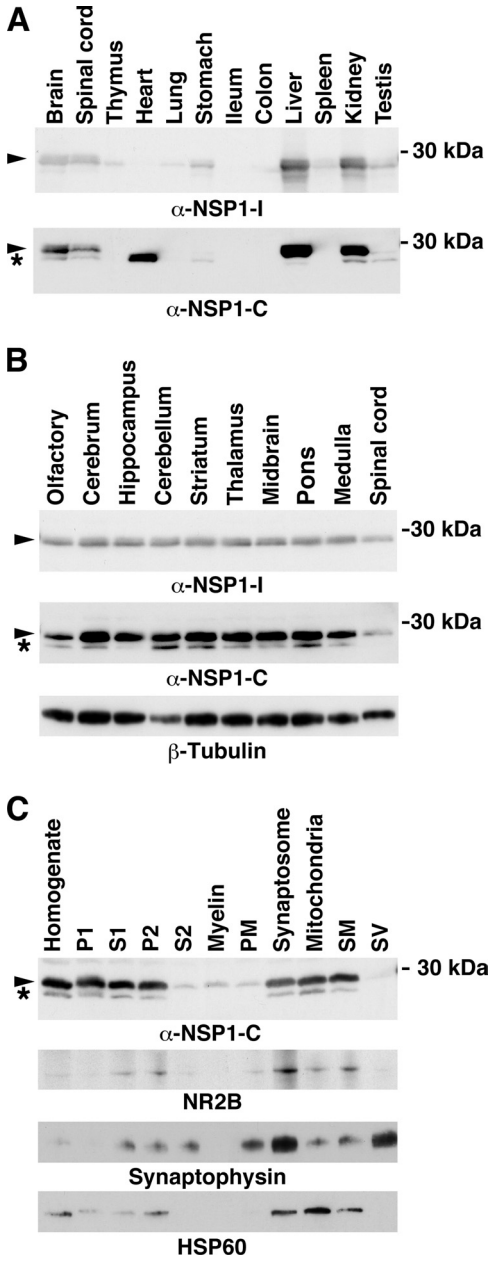

FIGURE 4. **Distribution of NIPSNAP1.** *A*, immunoblot analysis of NIPSNAP1. The homogenates of various mouse tissues were subjected to immunoblot analysis with anti-NSP1-I and anti-NSP1-C antibodies. *Arrowheads* indicate the mature form of NIPSNAP1, and the *asterisk*, NIPSNAP2. *B*, ubiquitous distribution of NIPSNAP1 in the central nervous system. The homogenates of various regions of the brain and spinal cord were subjected to immunoblot analysis with anti-NSP1-I, anti-NSP1-C, and anti-β-tubulin. *C*, subcellular distribution of NIPSNAP1. The homogenate of mouse brain was subjected to subcellular fractionation. Each fraction (12 μg of protein) was analyzed by immunoblotting with anti-NSP1-C, NR2B, synaptophysin, and HSP60 antibodies. These experiments were performed at least 3 times, and similar results were obtained. *P1*, nucleus and cell debris; *S1*, crude synaptosomal fraction; *P2*, crude synaptosomal pellet fraction; *S2*, cytosolic synaptosomal fraction; *PM*, plasma membrane fraction; *SM*, crude synaptic membrane fraction; *SV*, crude synaptic vesicle fraction.

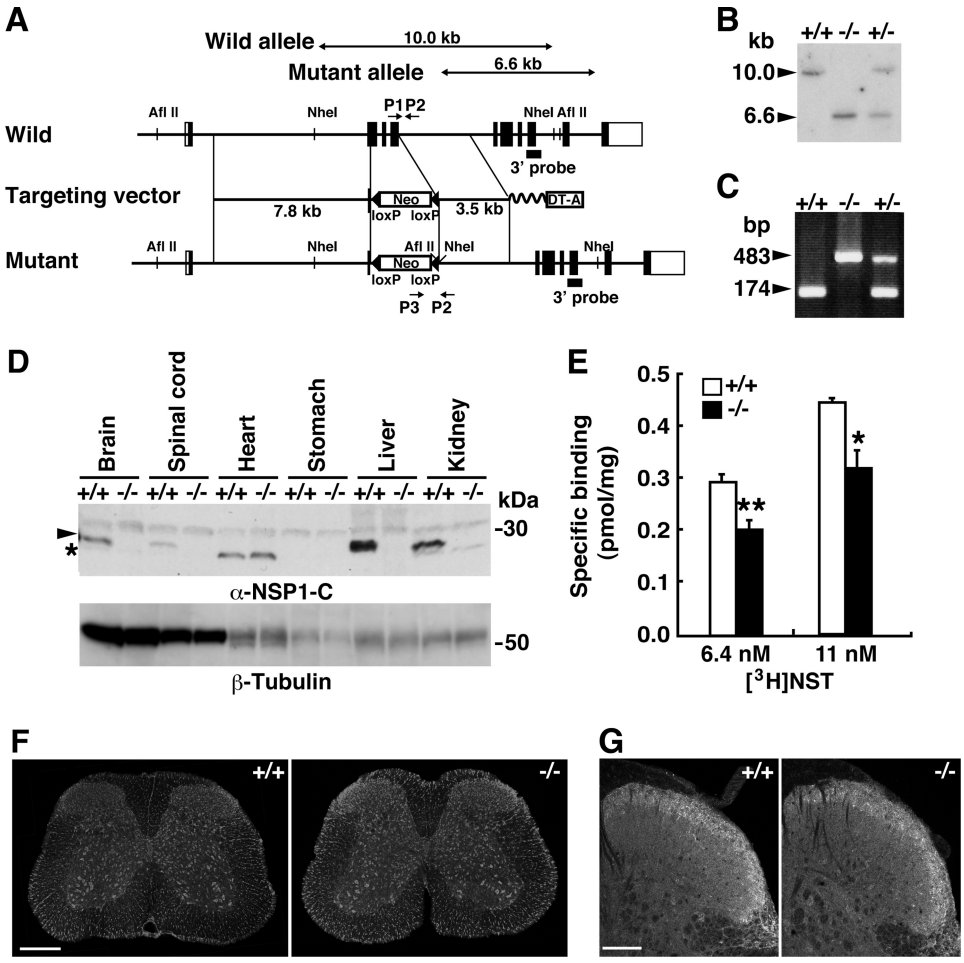

FIGURE 5. **Generation and characterization of NIPSNAP1$^{-/-}$ mice.** *A*, construction of the targeting vector. The wild-type allele of the NIPSNAP1 gene, targeting vector, and mutant allele are shown. Exons are represented by *boxes*. The neomycin resistance gene (*Neo*) and the gene coding for diphtheria toxin A (*DT-A*) are indicated. The probe used for Southern blot analysis in *B* is indicated by a *bold bar*; the locations of PCR primers used for genotyping in *C* are indicated by *arrows*; and NheI-digested fragments detected by the probe by *double-headed arrows*. *B*, Southern blot analysis of the mutant mice. NheI-cleaved tail DNA of wild-type (+/+), NIPSNAP1$^{-/-}$ (−/−), and heterozygous (+/−) littermates were hybridized with the probe indicated in *A* (10.0 kb for NIPSNAP1$^{+/+}$ and 6.6 kb for NIPSNAP1$^{-/-}$). *C*, PCR genotyping of the mutant mice. The wild-type allele band (174 bp) and the mutant allele band (483 bp) were amplified by PCR with the primers indicated in *A*. *D*, immunoblot analysis of the mutant mice. The homogenates of the adult tissues were immunoblotted with anti-NSP1-C antibody. The *arrowhead* indicates NIPSNAP1, and the *asterisk*, NIPSNAP2. *E*, [^{3}H]NST binding to the membrane fraction from spinal cord of the mutant mice. The membrane fraction was incubated with [^{3}H]NST (6.4 and 11 nM) at 30 °C for 60 min (mean ± S.E., $n = 3$). **, $p < 0.01$, *, $p < 0.05$ *versus* wild-type value. *F*, histological analysis of wild-type and NIPSNAP1$^{-/-}$ mice. Nissl staining of the spinal cord. *Bar*, 500 μm. *G*, fluorescence micrographs of the spinal dorsal horn of the mutant mice stained with anti-NST antibody. These experiments were performed at least 3 times, and similar results were obtained. *Bar*, 100 μm.

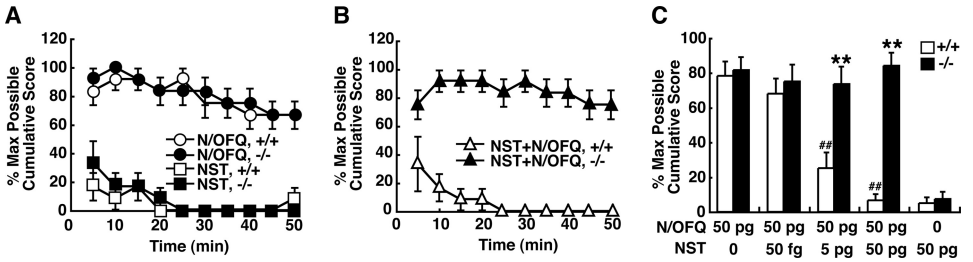

FIGURE 6. **Tactile allodynia induced by N/OFQ and NST in NIPSNAP1$^{-/-}$ mice.** *A*, N/OFQ (50 pg; ○, ●) or NST (500 pg; □, ■) was injected intrathecally into wild-type (+/+; ○, □) and NIPSNAP1$^{-/-}$ (−/−; ●, ■) mice. Allodynia was assessed once every 5 min for 50 min, and the values (mean ± S.E., $n = 6$) are expressed as % of the maximal possible cumulative score over the 50-min experimental period. *B*, NST (500 pg) and N/OFQ (50 pg) were simultaneously injected intrathecally into wild-type (△, +/+) and NIPSNAP1$^{-/-}$ (▲, −/−) mice. *C*, the values shown are expressed as a percent of the maximum possible cumulative score for allodynia over the 50-min observation period at the indicated concentration of NST and N/OFQ (mean ± S.E., $n = 5$). **, $p < 0.01$, *versus* wild-type value; ##, $p < 0.01$, N/OFQ-injected value in wild-type mice.

NIPSNAP1$^{+/+}$ mice, whereas the inhibition by NST disappeared in NIPSNAP1$^{-/-}$ mice (Fig. 6*C*). Taken together with no difference in NST immunoreactivity in the dorsal horn of spinal cord between wild-type and NIPSNAP1$^{-/-}$ mice (Fig. 5*G*), these results suggest that the inhibition of N/OFQ-evoked allodynia by NST is mediated by NIPSNAP1.

DISCUSSION

In the present study, we identified NIPSNAP1 as an NST-interacting protein. An N-terminal truncated mature form (29 kDa) of NIPSNAP1 was expressed in the brain, spinal cord, liver, and kidney *in vivo*; the full-length pre-protein of NIPSNAP1 was 33 kDa. The mature form of NIPSNAP1 was a membrane protein harboring an intracellular C-terminal region. NST is involved in several central nervous functions including pain transmission. The inhibition of N/OFQ-evoked allodynia by NST was abolished in NIPSNAP1-deficient mice. These results demonstrate that NIPSNAP1, as an NST-interacting protein, is an important molecule for the regulation of pain transmission via NST.

First, NIPSNAP1 is thought to contribute to vesicular trafficking, because the gene for NIPSNAP1 in *C. elegans* is present in a polycistronic operon encoding 4-nitrophenylphosphatase and non-neuronal SNAP25-like proteins (1). Regarding the NIPSNAP family, NIPSNAP2, a highly homologous protein of NIPSNAP1 with 75% amino acid identity, is expressed in glioblastoma and cell lines co-amplified with the epidermal growth factor receptor gene, besides being found in normal tissues such as lung and skeletal muscle (29). NIPSNAP4 (annotated as TassC, target for *Salmonella* secreted protein C) was first identified, by use of the yeast two-hybrid assay, as a host cell target for the *Salmonella* virulence protein SpiC (30). SpiC interferes with intracellular trafficking in host cells of the *Salmonella* strain in NIPSNAP4-deficient macrophages. NIPSNAP4 is found in lipid rafts of membrane (31) and mitochondria (32). Mitochondrial NIPSNAP4 interacts with inhibitor of apoptosis proteins, which suppress apoptosis by binding to and inhibiting active caspases, and it is able to antagonize the X-linked inhibitor of apoptosis protein-induced inhibition of caspase 3 *in vitro* (32). Recent reports suggest that NIPSNAP1 interacts with the transient receptor potential vanilloid channel (TRPV) 6 (33), the amyloid precursor protein (8), and the branched-chain α-ketoacid dehydrogenase enzyme complex (9). Here, the following lines of evidence led us to conclude that NIPSNAP1 is an NST-interacting protein: 1) the mature form of NIPSNAP1 (29 kDa) and its immunoreactive proteins (28 and 27 kDa) were isolated from synaptosomal membrane fractions of mouse spinal cord by use of NST-conjugated SG beads (Figs. 1*A* and 2*E*); 2) [^{3}H]NST specifically bound to the membrane fraction of NIPSNAP1-transfected COS-7 cells (Fig. 1, *F–H*); 3) [^{3}H]NST binding to the synaptosomal membrane of spinal cord was significantly reduced in NIPSNAP1$^{-/-}$ mice (Fig. 5*E*); and 4) the inhibition of N/OFQ-induced allodynia by NST was abolished in NIPSNAP1$^{-/-}$ mice (Fig. 6). Because NIPSNAP2 is highly homologous to NIPSNAP1, NST may also bind NIPSNAP2. [^{3}H]NST tended to bind to NIPSNAP2 expressed in COS-7 cells, and the B_{max} value of NIPSNAP2 was approximately half (53.4%) of NIPSNAP1 (Fig. 1*G*). Fig. 2*B* shows that the expression of NIPSNAP2 was ~2.9-fold lower than that of NIPSNAP1, assuming that the anti-NSP1-C antibody had the same affinity for NIPSNAP1 and NIPSNAP2. Hence, the difference of B_{max} values between NIPSNAP1 and NIPSNAP2 does not negate dependence of the expression level. On the other hand, the K_d value of [^{3}H]NST binding in NIPSNAP2-transfected COS-7 cells was 10.6 nM, which was 1.8-fold lower compared with NIPSNAP1 (5.8 nM). NST-conjugated SG beads bound the cell membranes transfected with NIPSNAP1 but not NIPSNAP2 (Fig. 1*D*). These results suggest NIPSNAP1 has a higher affinity for NST than NIPNSAP2.

NIPSNAP1 is found to be localized in the mitochondria in rat liver and NIPSNAP1-transfected COS-7 cells, and the mitochondrial NIPSNAP1 forms complex with the branched-chain α-ketoacid dehydrogenase enzyme complex and the amyloid precursor protein (8, 9). In contrast, the NIPSNAP1 protein is localized in the postsynaptic density fraction of mouse forebrains (6). NIPSNAP1 also binds the cell surface protein, such as a highly selective Ca^{2+} channel TRPV6, and inhibits TRPV6 activity (33). The NIPSNAP1 immunoreactivity in the pyramidal neurons of cerebral cortex is detected in the periphery area, in addition to the perinuclear area rich in mitochondria (9). Consistent with these reports, Fig. 4*C* revealed the similar density of NIPSNAP1 in both mitochondria and synaptic membranes, but the density of a mitochondrial marker HSP60 in mitochondria was 1.6-fold higher than in synaptic membranes. Hence, the discrepant ratio between NIPSNAP1 and HSP60 suggests that NIPSNAP1 was localized in not only mitochondria but also synaptic membranes. Furthermore, the mature form of NIPSNAP1 (29 kDa) was expressed on the cell surface, as revealed by analysis of biotinylated cell surface protein and immunofluorescence analysis (Fig. 3). The NST-conjugated SG beads bound the mature form of NIPSNAP1 (29 kDa) and its immunoreactive proteins (28 and 27 kDa) in NIPSNAP1-expressing COS-7 cells and the synaptosomal membrane of mouse spinal cord (Fig. 2, *D* and *E*). These results suggest that NST binds to at least the mature form of NIPSNAP1 probably localized at the cell surface.

NST inhibits N/OFQ-induced pain transmission such as allodynia and hyperalgesia (12–14), inflammatory pain responses (15–17), and morphine tolerance (18, 19). The mature form of NIPSNAP1 was expressed in various regions of the brain and spinal cord (Fig. 4, *A* and *B*). The inhibition of N/OFQ-evoked allodynia by NST seen in wild-type mice was completely lacking in NIPSNAP1$^{-/-}$ mice (Fig. 6). However, specific [^{3}H]NST binding in the spinal cord membrane fraction of NIPSNAP1$^{-/-}$ mice was reduced by ~30%, but not completely (Fig. 5*E*). NST may bind other protein(s) in the spinal cord besides NIPSNAP1. Heretofore, the possibility that NST acts through an as yet unidentified G protein-coupled receptor is suggested by the findings that NST suppresses inhibitory neurotransmission in the rat spinal cord *in vitro* (20), inhibits 5-hydroxytryptamine release in the mouse neocortex *in vitro* (34), and induces nociception *in vivo* (22), all of which are sensitive to a $G_{i/o}$ protein inhibitor, pertussis toxin. Furthermore, NST depolarizes central amygdala nucleus-periaqueductal gray neurons by causing the opening of canonical transient receptor potential cation channels via pertussis toxin-insensitive $G_{q/11}$ (35). NST increases the cytosolic free Ca^{2+} concentration ($[Ca^{2+}]_i$) in primary culture cells from rat embryonic spinal cord.[3] However, NST did not increase $[Ca^{2+}]_i$ in COS-7 cells

[3] E. Okuda-Ashitaka and S. Ito, unpublished data.

transfected with NIPSNAP1 (data not shown), suggesting that NIPSNAP1 did not influence the $[Ca^{2+}]_i$ induced by NST directly. Taken together that NIPSNAP1 is a membrane protein containing a single transmembrane segment but not seven transmembrane segments (Fig. 2*A*), NIPSNAP1 may be involved in a novel mechanism of pain transmission regulated by NST independent of a signal pathway acting through a G protein-coupled receptor.

In the brain, the mature form of NIPSNAP1 was distributed in various brain regions (Fig. 4*B*). NIPSNAP1 is found in neuron but not glial cells such as astrocyte and oligodendrocyte, in particular pyramidal neurons in the cerebral cortex, glutamatergic neurons of the granule cell layer, and γ-aminobutyric acidergic of the polymorphic layer in the hippocampus, dopaminergic neurons in the midbrain, noradrenergic neurons in the brainstem, Purkinje neurons in the cerebellum, and motor neurons in the spinal cord (9). Furthermore, the NIPSNAP1 protein level is increased during generalized seizures caused by kainite (6), and the NIPSNAP1 mRNA level is reduced in the brain of a mouse model for phenylketonuria, an inborn error of amino acid metabolism caused by phenylalanine hydroxylase deficiency (7). Also, NIPSNAP1 binds molecules bearing maple syrup urine disease (9) and Alzheimer disease (8). We demonstrated here that NIPSNAP1-deficient mice abolished the inhibition of N/OFQ-evoked allodynia by NST (Fig. 6). Thus, NIPSNAP1 may be involved in several central functions containing pain transmission. In accord with the interaction of NIPSNAP1 and membrane protein TRPV6, NIPSNAP1 might bind a signal molecule, a channel, and a receptor involving pain transmission, and NST probably regulates the interaction. Further studies focusing on the relationship between NST and NIPSNAP1 will contribute to our better understanding of pain transmission evoked by NST. One of the physiological functions of NIPSNAP1 is the pain modulation, and it may provide a novel therapeutic target for pathological pain.

REFERENCES

1. Seroussi, E., Pan, H. Q., Kedra, D., Roe, B. A., and Dumanski, J. P. (1998) Characterization of the human NIPSNAP1 gene from 22q12. A member of a novel gene family. *Gene.* **212,** 13–20
2. Satoh, K., Takeuchi, M., Oda, Y., Deguchi-Tawarada, M., Sakamoto, Y., Matsubara, K., Nagasu, T., and Takai, Y. (2002) Identification of activity-regulated proteins in the postsynaptic density fraction. *Genes Cells* **7,** 187–197
3. Surendran, S., Tyring, S. K., and Matalon, R. (2005) Expression of calpastatin, minopontin, NIPSNAP1, rabaptin-5 and neuronatin in the phenylketonuria (PKU) mouse brain. Possible role on cognitive defect seen in PKU. *Neurochem. Int.* **46,** 595–599
4. Tummala, H., Li, X., and Homayouni, R. (2010) Interaction of a novel mitochondrial protein, 4-nitrophenylphosphatase domain and non-neuronal SNAP25-like protein homolog 1 (NIPSNAP1), with the amyloid precursor protein family. *Eur. J. Neurosci.* **31,** 1926–1934
5. Nautiyal, M., Sweatt, A. J., MacKenzie, J. A., Mark Payne, R., Szucs, S., Matalon, R., Wallin, R., and Hutson, S. M. (2010) Neuronal localization of the mitochondrial protein NIPSNAP1 in rat nervous system. *Eur. J. Neurosci.* **32,** 560–569
6. Shimizu, N., Sugimoto, K., Tang, J., Nishi, T., Sato, I., Hiramoto, M., Aizawa, S., Hatakeyama, M., Ohba, R., Hatori, H., Yoshikawa, T., Suzuki, F., Oomori, A., Tanaka, H., Kawaguchi, H., Watanabe, H., and Handa, H. (2000) High-performance affinity beads for identifying drug receptors. *Nat. Biotechnol.* **18,** 877–881
7. Ohtsu, Y., Ohba, R., Imamura, Y., Kobayashi, M., Hatori, H., Zenkoh, T., Hatakeyama, M., Manabe, T., Hino, M., Yamaguchi, Y., Kataoka, K., Kawaguchi, H., Watanabe, H., and Handa, H. (2005) Selective ligand purification using high-performance affinity beads. *Anal. Biochem.* **338,** 245–252
8. Okuda-Ashitaka, E., Minami, T., Tachibana, S., Yoshihara, Y., Nishiuchi, Y., Kimura, T., and Ito, S. (1998) Nocistatin, a peptide that blocks nociceptin action in pain transmission. *Nature* **392,** 286–289
9. Okuda-Ashitaka, E., and Ito, S. (2000) Nocistatin, a novel neuropeptide encoded by the gene for the nociceptin/orphanin FQ precursor. *Peptides* **21,** 1101–1109
10. Ito, S., Okuda-Ashitaka, E., Imanishi, T., and Minami, T. (2000) Central roles of nociceptin/orphanin FQ and nocistatin. Allodynia as a model of neural plasticity. *Prog. Brain Res.* **129,** 205–218
11. Nakagawa, T., Kaneko, M., Inamura, S., and Satoh, M. (1999) Intracerebroventricular administration of nocistatin reduces inflammatory hyperalgesia in rats. *Neurosci. Lett.* **265,** 64–66
12. Yamamoto, T., and Sakashita, Y. (1999) Effect of nocistatin and its interaction with nociceptin/orphanin FQ on the rat formalin test. *Neurosci. Lett.* **262,** 179–182
13. Nakano, H., Minami, T., Abe, K., Arai, T., Tokumura, M., Ibii, N., Okuda-Ashitaka, E., Mori, H., and Ito, S. (2000) Effect of intrathecal nocistatin on the formalin-induced pain in mice *versus* that of nociceptin/orphanin FQ. *J. Pharmacol. Exp. Ther.* **292,** 331–336
14. Sun, R. Q., Zhao, C. S., Wang, H. J., Jing, Z., Wang, W., Yang, K., Wang, Y., Chang, J. K., and Han, J. S. (2001) Nocistatin, a peptide reversing acute and chronic morphine tolerance. *Neuroreport* **12,** 1789–1792
15. Ge, Z. J., Li, C., Zhang, L. C., Zeng, Y. M., Cao, J. L., Dai, T. J., Wang, J. K., Cui, G. X., Tan, Y. F., Zhao, Y. P., and Liu, G. J. (2007) Involvement of local orphanin FQ in the development of analgesic tolerance induced by morphine microinjections into the dorsal raphe nucleus of rats. *Neurosci. Lett.* **413,** 233–237
16. Zeilhofer, H. U., Selbach, U. M., Guhring, H., Erb, K., and Ahmadi, S. (2000) Selective suppression of inhibitory synaptic transmission by nocistatin in the rat spinal cord dorsal horn. *J. Neurosci.* **20,** 4922–4929
17. Ahmadi, S., Muth-Selbach, U., Lauterbach, A., Lipfert, P., Neuhuber, W. L., and Zeilhofer, H. U. (2003) Facilitation of spinal NMDA receptor currents by spillover of synaptically released glycine. *Science* **300,** 2094–2097
18. Inoue, M., Kawashima, T., Allen, R. G., and Ueda, H. (2003) Nocistatin and prepro-nociceptin/orphanin FQ 160–187 cause nociception through activation of $G_{i/o}$ in capsaicin-sensitive and of G_s in capsaicin-insensitive nociceptors, respectively. *J. Pharmacol. Exp. Ther.* **306,** 141–146
19. Hiramatsu, M., and Inoue, K. (1999) Effects of nocistatin on nociceptin-induced impairment of learning and memory in mice. *Eur. J. Pharmacol.* **367,** 151–155
20. Olszewski, P. K., Shaw, T. J., Grace, M. K., Billington, C. J., and Levine, A. S. (2000) Nocistatin inhibits food intake in rats. *Brain. Res.* **872,** 181–187
21. Gavioli, E. C., Rae, G. A., Calo', G., Guerrini, R., and De Lima, T. C. (2002) Central injections of nocistatin or its C-terminal hexapeptide exert anxiogenic-like effect on behavior of mice in the plus-maze test. *Br. J. Pharmacol.* **136,** 764–772
22. Kamei, J., Matsunawa, Y., Miyata, S., Tanaka, S., and Saitoh, A. (2004) Effects of nociceptin on the exploratory behavior of mice in the hole-board test. *Eur. J. Pharmacol.* **489,** 77–87
23. Dunah, A. W., and Standaert, D. G. (2001) Dopamine D1 receptor-dependent trafficking of striatal NMDA glutamate receptors to the postsynaptic membrane. *J. Neurosci.* **21,** 5546–5558
24. Ueda, T., Greengard, P., Berzins, K., Cohen, R. S., Blomberg, F., Grab, D. J., and Siekevitz, P. (1979) Subcellular distribution in cerebral cortex of two proteins phosphorylated by a cAMP-dependent protein kinase. *J. Cell Biol.* **83,** 308–319
25. Murata, T., Furushima, K., Hirano, M., Kiyonari, H., Nakamura, M., Suda, Y., and Aizawa, S. (2004) *ang* is a novel gene expressed in early neuroectoderm, but its null mutant exhibits no obvious phenotype. *Gene. Expr. Patterns* **5,** 171–178
26. Yagi, T., Tokunaga, T., Furuta, Y., Nada, S., Yoshida, M., Tsukada, T., Saga, Y., Takeda, N., Ikawa, Y., and Aizawa, S. (1993) A novel ES cell

line, TT2, with high germline-differentiating potency. *Anal. Biochem.* **214,** 70–76
27. Zimmermann, M. (1983) Ethical guidelines for investigations of experimental pain in conscious animals. *Pain* **16,** 109–110
28. Okuda-Ashitaka, E., Tachibana, S., Houtani, T., Minami, T., Masu, Y., Nishi, M., Takeshima, H., Sugimoto, T., and Ito, S. (1996) Identification and characterization of an endogenous ligand for opioid receptor homologue ROR-C. Its involvement in allodynic response to innocuous stimulus. *Mol. Brain. Res.* **43,** 96–104
29. Wang, X. Y., Smith, D. I., Liu, W., and James, C. D. (1998) GBAS, a novel gene encoding a protein with tyrosine phosphorylation sites and a transmembrane domain, is co-amplified with EGFR. *Genomics* **49,** 448–451
30. Lee, A. H., Zareei, M. P., and Daefler, S. (2002) Identification of a NIPSNAP homologue as host cell target for *Salmonella* virulence protein SpiC. *Cell Microbiol.* **4,** 739–750
31. Buechler, C., Bodzioch, M., Bared, S. M., Sigruener, A., Boettcher, A., Lapicka-Bodzioch, K., Aslanidis, C., Duong, C. Q., Grandl, M., Langmann, T., Dembinska-Kiec, A., and Schmitz, G. (2004) Expression pattern and raft association of NIPSNAP3 and NIPSNAP4, highly homologous proteins encoded by genes in close proximity to the ATP-binding cassette transporter A1. *Genomics* **83,** 1116–1124
32. Verhagen, A. M., Kratina, T. K., Hawkins, C. J., Silke, J., Ekert, P. G., and Vaux, D. L. (2007) Identification of mammalian mitochondrial proteins that interact with IAPs via N-terminal IAP binding motifs. *Cell Death Differ.* **14,** 348–357
33. Schoeber, J. P., Topala, C. N., Lee, K. P., Lambers, T. T., Ricard, G., van der Kemp, A. W., Huynen, M. A., Hoenderop, J. G., and Bindels, R. J. (2008) Identificaion of NIPSNAP1 as a novel auxiliary protein inhibiting TRPV6 activity. *Eur. J. Physiol.* **457,** 91–101
34. Fantin, M., Fischetti, C., Trapella, C., and Morari, M. (2007) Nocistatin inhibits 5-hydroxytryptamine release in the mouse neocortex via presynaptic $G_{i/o}$ protein-linked pathways. *Br. J. Pharmacol.* **152,** 549–555
35. Chen, Y. L., Li, A. H., Yeh, T. H., Chou, A. H., and Wang, H. L. (2009) Nocistatin and nociceptin exert opposite effects on the excitability of central amygdala nucleus-periaqueductal gray projection neurons. *Mol. Cell. Neurosci.* **40,** 76–88